PROTEINS: Structure, Function, and Genetics 16:311–326 (1993)

RESEARCH ARTICLES

Structures of the "Open" and "Closed" State of Trypanosomal Triosephosphate Isomerase, as Observed in a New Crystal Form: Implications for the Reaction Mechanism

Martin E.M. Noble, Johan Ph. Zeelen, and Rik K. Wierenga
European Molecular Biology Laboratory, D-6900 Heidelberg, Germany

ABSTRACT **The structure of trypanosomal triosephosphate isomerase (TIM) has been solved at a resolution of 2.1Å in a new crystal form grown at pH 8.8 from PEG6000. In this new crystal form (space group *C*2, cell dimensions 94.8 Å, 48.3 Å, 131.0 Å, 90.0°, 100.3°, 90.0°), TIM is present in a ligand-free state. The asymmetric unit consists of two TIM subunits. Each of these subunits is part of a dimer which is sitting on a crystallographic twofold axis, such that the crystal packing is formed from two TIM dimers in two distinct environments. The two constituent monomers of a given dimer are, therefore, crystallographically equivalent. In the ligand-free state of TIM in this crystal form, the two types of dimer are very similar in structure, with the flexible loops in the "open" conformation. For one dimer (termed molecule-1), the flexible loop (loop-6) is involved in crystal contacts. Crystals of this type have been used in soaking experiments with 0.4 M ammonium sulphate (studied at 2.4 Å resolution), and with 40 μM phosphoglycolohydroxamate (studied at 2.5 Å resolution). It is found that transfer to 0.4 M ammonium sulphate (equal to 80 times the Ki of sulphate for TIM), gives rise to significant sulphate binding at the active site of one dimer (termed molecule-2), and less significant binding at the active site of the other. In neither dimer does sulphate induce a "closed" conformation. In a mother liquor containing 40 μM phosphoglycolohydroxamate (equal to 10 times the Ki of phosphoglycolohydroxamate for TIM), an inhibitor molecule binds at the active site of only that dimer of which the flexible loop is free from crystal contacts (molecule-2). In this dimer, it induces a closed conformation. These three structures are compared and discussed with respect to the mode of binding of ligand in the active site as well as with respect to the conformational changes resulting from ligand binding.** © 1993 Wiley-Liss, Inc.

Key words: triosephosphate isomerase, TIM, X-ray crystallography, binding studies, crystal packing, conformational change, reaction mechanism

INTRODUCTION

Triosephosphate isomerase (TIM) is an enzyme for which considerable amounts of biochemical and structural data have been collected. This data has been used to develop a detailed picture of the mechanism and structural properties of this ubiquitous glycolytic enzyme, which catalyzes the interconversion of dihydroxyacetone phosphate and D-glyceraldehyde-3-phosphate. TIM is functional as a homodimeric molecule, with subunits each containing around 250 residues. X-ray crystallographic studies, initially performed on the enzyme from chicken muscle,[1] and subsequently from yeast[2] and from trypanosome,[3] have shown that each monomer is folded as a regular structure formed from an eightfold repeat of a (loop-β-loop-α) motif. The eight β-strands (termed β1–β8) form a parallel β-barrel surrounded by a coat of eight α-helices (termed α1–α8). Since the original observation of this fold in triosephosphate isomerase, it has been found in proteins serving 20 different functions.[4] TIM itself has its active site at the C-terminal end of the β-barrel, with catalytic

Abbreviations: TIM, triosephosphate isomerase (E.C.5.3.1.1.); NMR, nuclear magnetic resonance; DHAP, dihydroxyacetone phosphate; GAP, D-glyceraldehyde-3-phosphate; EDTA, ethylenediaminetetraacetic acid; DTT, dithiothreitol; PEG, polyethyleneglycol; MES, 2-[N-morpholino]ethanesulphonic acid; G3P, glycerol-3-phosphate; PGH, phosphoglycolohydroxamate; rms, root-mean-square.

Received October 6, 1992; revision accepted March 1, 1993.
Address reprint requests to Dr. Rik K. Wierenga, European Molecular Biology Laboratory, Meyerhofstrasse 1, D-6900 Heidelberg, Germany.
Martin E.M. Noble's new address is Laboratory of Molecular Biophysics, University of Oxford, South Parks Road, Oxford OX1 3QU, England.

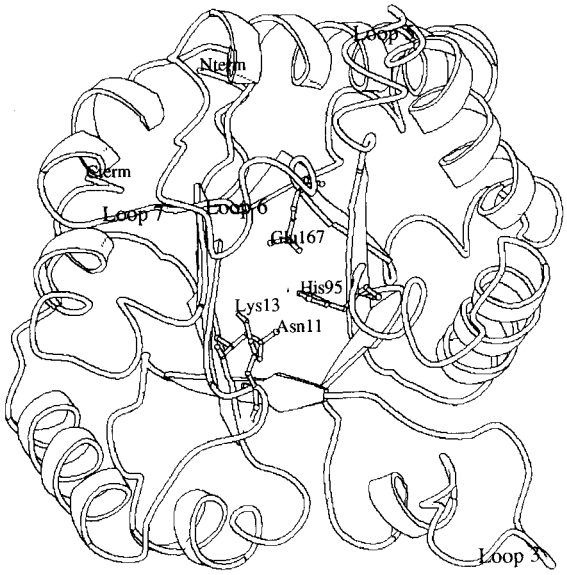

Fig. 1. Line drawing of one monomer of triosephosphate isomerase. The eightfold repeat of a (loop-β-loop-α) motif is viewed along the barrel axis from the C-terminal end of the β-strands. The explicitly drawn and labeled residues (Asn11, Lys13, His95, and Glu167) all form hydrogen bonds with bound substrate analogues. Also labeled are loops 5 (residues 129–139), 6 (residues 167–180), and 7 (residues 210–214). These loops, which are known to undergo conformational changes upon ligand binding, are depicted in their "closed" conformation. Loop-3 (residues 70–80), which is also labeled, is responsible for many of the contacts between monomers of the dimeric enzyme. This picture was generated using the program XRENDER (Noble, M.E.M., unpublished results).

residues contributed by the β-strands, and the loops connecting β-strands to subsequent α-helices (termed loops 1–8) (Fig. 1). Trypanosomal TIM has 249 residues, numbered 2–250, and the numbering in this paper will relate to the sequence of trypanosomal TIM. The equivalent residues of chicken TIM and yeast TIM can be deduced from the sequence alignment given in Figure 2.

The catalytic cycle of TIM, which is rate-limited by the diffusive substrate approach step,[5] involves initially a binding stage in which a number of structural changes are required of the protein. These stuctural changes were first observed in substrate soaking experiments performed on chicken TIM,[6] and have since been studied at higher resolution on substrate analogue complexes achieved by soaking experiments carried out on TIM from trypanosomes,[7–9] and cocrystallization, in the case of TIM from yeast.[10,11] These structural changes involve a major movement of loop-6 residues 167–180, the "flexible" loop, and coordinated movements of the neighboring loops, loop-5 (residues 129–135), and loop 7 (residues 210–214).[12] The residues at the tip of loop-6 (I172-G173-T174-G175) appear to move as a rigid body, to close off the active site from solvent.[12,13] The largest CA coordinate difference between "open" and "closed" states is around 7 Å (for residue Thr174). The rigidity of residues at the tip of loop-6 derives in part from hydrogen bonds formed in both the open and closed state from OG1 of Thr 174 to residues nearby on the loop (O of Trp170 and N of Thr174 towards the N-terminus, and N of Gly175 and N of Lys176 towards the C-terminus). It has been shown that deletion of the flexible loop leads to an increase in the rate of a phosphate elimination side reaction of TIM, and in a decreased stabilization of the transition states for proton abstraction.[14]

Chicken TIM, crystallized from 2.4 M ammonium sulphate, and solved at a resolution of 2.5 Å, has a sulphate bound at each of the two active sites (sulphate is a competitive inhibitor of TIM, with a K_i of 5 mM[15]). The crystallographic asymmetric unit in this case contains a dimer. The flexible loops of the two monomers of chicken TIM are either impossible to trace, in the case of subunit-1, or poorly defined in the open conformation, in the case of subunit-2. The native structure of trypanosomal TIM grown from 2.4 M ammonium sulphate (referred to as the "2.4MAS" structure) also has a dimer in the asymmetric unit.[3] In the case of subunit-1, a glutamate from a crystallographically related molecule protrudes into the active site, near to the position where sulphate would be expected to bind, and the flexible loop is constrained by crystal contacts to maintain the open conformation. For these reasons, the active site is devoid of ligand. By contrast, the active site and flexible loop of subunit-2 are free, and a sulphate molecule is bound. This sulphate is coordinated by a main chain nitrogen of the flexible loop, which occupies a conformation referred to as "almost closed." This name is chosen because a further closed state, referred to as the "closed" state, has also been characterized, differing maximally in CA position by about 1Å in the flexible loop region.[7]

The flexible loop of subunit-2 can be induced to adopt either the open or the fully closed conformation by soaking sulphate out of the crystals,[12] or by soaking either substrate analogues or inorganic phosphate into the crystals,[7–9] respectively. In the almost closed conformation, the atomic B-factors of the flexible loop are high, consistent with either partial occupancy of the closed state, or limited flexibility around the mean conformation. In the fully closed state, the atomic B-factors are low.

Structures of trypanosomal TIM and yeast TIM in complex with substrate or transition state analogues also have shown variability of the conformation of the glutamate residue thought to be responsible for proton abstraction (Glu167 in trypanosomal TIM). This residue has two stable conformations with low B-factors termed "swung-out," and "swung-in." The swung-out conformation is observed in ligand-free structures. In this conformation, the side chain has a combination of torsion angles frequently

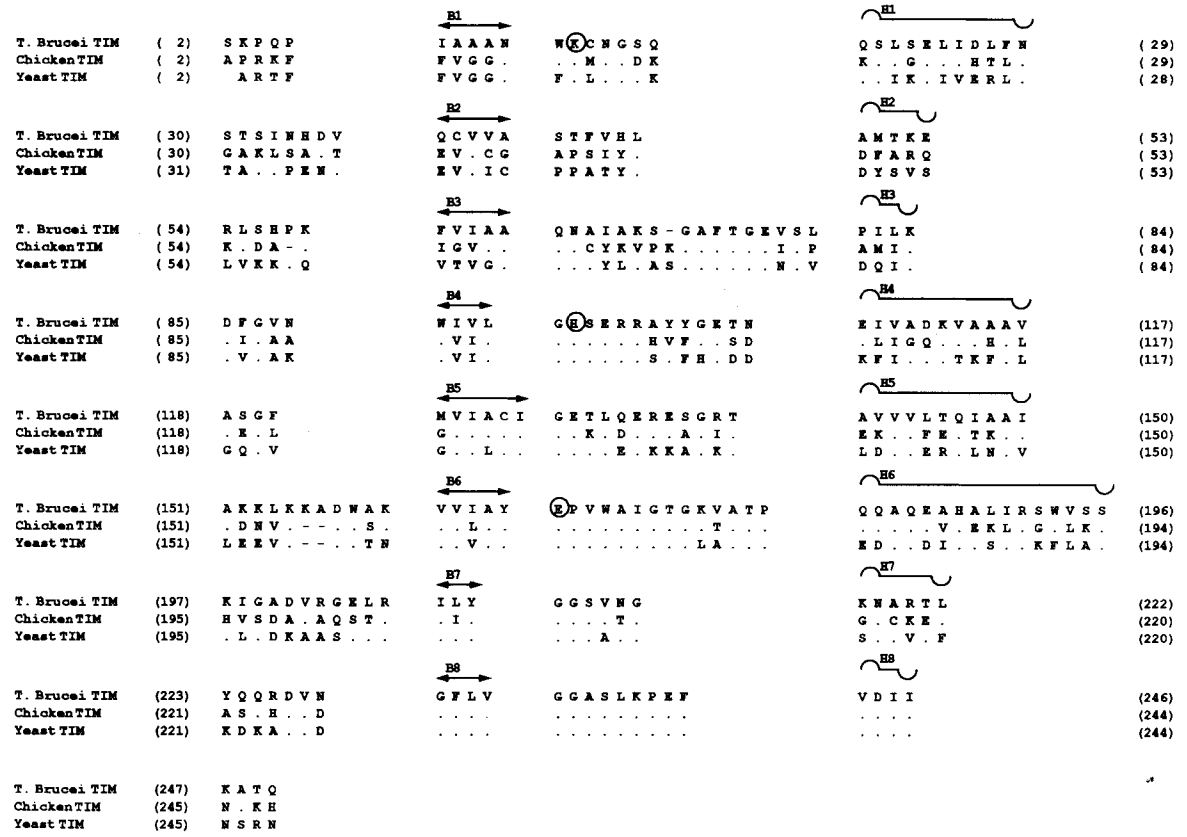

Fig. 2. The sequences of trypanosomal TIM, chicken TIM, and yeast TIM. The β-strands and α-helices of the eight (βα)-units are specifically indicated. The catalytic residues Lys13, His95, and Glu167 are encircled.

observed in the database of well refined structures ($\chi^1 = -58$, $\chi^2 = -175$) and the carboxylate group forms hydrogen bonds with OG(Ser96) and N(Ser96). The swung-in conformation is observed in complexes between TIM and the ligands phosphate,[8] glycerol-3-phosphate (G3P),[7] 3-phosphonopropionate,[7] phosphoglycolohydroxamate (PGH),[11] or 2-phosphoglycollate.[10] This conformation has similar side chain torsion angles to the "swung-out" conformation, but a different main chain conformation, associated with closure of the flexible loop. As a result, the carboxylate group occupies a different position, appropriate for its assumed catalytic role, interacting with atoms of the ligand (for ligands other than phosphate or sulphate). A third conformational state of the glutamate side chain is observed in the complex with either sulphate,[3] 2-phosphoglycerate,[9] or 3-phosphoglycerate.[7] This conformation has the backbone conformation of the swung-in state, but the carboxylate position of the swung-out state. This is achieved by having an unusual and strained combination of side chain torsion angles, and correspondingly the B-factors of the side chain atoms are high.

The mechanism of the TIM reaction is believed to involve abstraction of a proton from C3 of DHAP by the catalytic glutamate residue, giving rise to a negatively charged enediolate intermediate, followed by exchange of protons between the substrate oxygens (O6 to O5, Fig. 3), and readdition of a proton to C2. This is summarized in Figure 3, where the structural formula of the intermediate analogue PGH is also presented for comparison.

Differences in the nature of the sulphate bound state between TIM from chicken and trypanosome raise the question of the extent to which the crystalline environment might have affected the ligand binding properties, and the ligand-bound conformation of TIM. This question has been addressed by solving the structure of trypanosomal TIM in a different space group to that in which previous ligand-free and ligand-bound structures have been solved. The structure of trypanosomal TIM in this crystal form, grown from PEG6000, has been solved free from ligand, (termed PEG-native), after soaking with 0.4 M ammonium sulphate (termed PEG-SO4), and after soaking in 40 μM of the transition state analogue phosphoglycolohydroxamate (termed PEG-PGH). The structures of TIM in this new crystal form are compared with previous structures of trypanosomal TIM with similar ligands and the implications for the reaction mechanism are discussed.

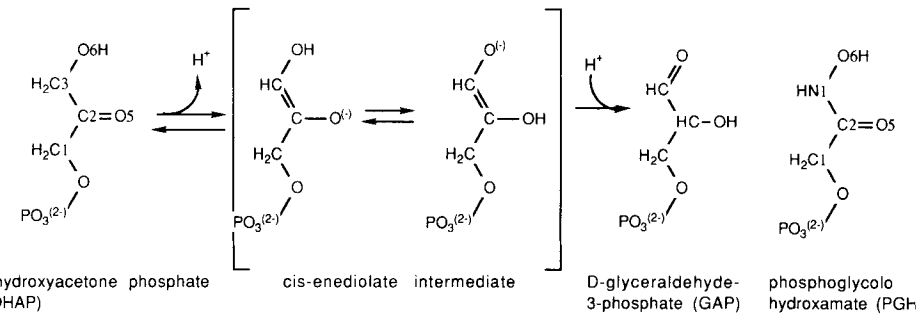

Fig. 3. The reaction mechanism of triosephosphate isomerase, and the structural formula of the intermediate analogue phosphoglycolohydroxamate.

MATERIALS AND METHODS

Crystallization and Data Collection

Recombinant trypanosomal TIM, prepared as described elsewhere,[16] was dissolved at a concentration of 5 mg.ml^{-1} in 25 mM Tris/HCl pH 7.6, containing also 20 mM NaCl, 50 mM ammonium sulphate, and 1 mM of each of EDTA, DTT, and NaN_3. Crystals were grown at room temperature using the hanging drop vapor diffusion technique, against a well solution containing 18% PEG6000 dissolved in 200 mM Tris/HCl pH 8.8, and 1 mM DTT, EDTA, and NaN_3. Crystals of a size up to 0.2 $\times$ 0.2 $\times$ 0.8 mm^3 grew within a week, and one of these was used to collect a dataset. Data were collected on a FAST area detector mounted on an Elliott GX21 rotating anode. Diffraction of the crystal extended to 2.0 Å resolution, and data collection was planned to provide a 2.1 Å dataset. Data collection was carried out using the program MADNES,[17] profile fitting with the XDS package,[18] and final scaling and merging with programs of the Groningen BIOMOL package. Statistics describing data quality are given in Table I. MADNES was used to identify the space group as $C2$, with the cell volume of 5.90 $\times$ 10^5 Å^3 giving a V_m of 5.5 Å^3.Da^{-1} for one subunit in the asymmetric unit, or 2.7 Å^3.Da^{-1} for two. On this basis, it was decided that the asymmetric unit contained two subunits.

Structure Solution by Molecular Replacement

Molecular replacement was performed using a dimer of the 2.4MAS structure. Structure factors were calculated in a large (128 $\times$ 128 $\times$ 128 Å^3) $P1$ cell, and the fast rotation function[19] was calculated with the program ALMN from the CCP4 suite.[20] A resolution range of 6.0–4.0 Å was chosen for included data, with Patterson integration limits of 25.0–3.0 Å, and beta sections running from 0° to 180° in steps of 2.5°. Four large peaks were observed in the resulting rotation function, two of height 16 standard deviations, and two of height 14 standard deviations. Within each pair of peaks of similar magnitude, the peaks were related by a 180° rotation around the b-axis. The rotation corresponding to the first solution was applied to the search model, and the rotated dimer was translated to have its center of mass on the origin. This model was then used in calculation of the T2 translation function,[21] using the programs GENSFC, CADLCF, TFSGEN, and FFTKW, of the CCP4 suite. Since $C2$ is a polar space group, only a single section was needed to determine the position of the model in the ac plane. This produced one very clear peak (5.9 σ, where peak height is described as standard deviations above the mean value) at a translation of (0,0). In space group $C2$, this position corresponds to the location of a crystallographic twofold axis.

The above observations suggested that in this case the asymmetric unit was formed of two monomers from distinct dimers rather than a single molecular dimer. Therefore, the rotation corresponding to the 14 σ peak in the rotation function was applied to the original search model, to provide a model which was translated to the origin before being used to calculate a second translation function. The result of this calculation was again a clear peak (5.4 σ), this time corresponding to a translation vector of (0,1/2) in the ac plane. As would be expected, this vector corresponds to a translation to another two fold axis of the $C2$ space group.

In this fashion, the location of the two monomers in the ac plane was determined. It remained necessary, however, to determine the relative b-coordinate of the two different molecules. This was achieved by means of an R-factor search, with one monomer at a fixed position, and the other translated in steps of 0.04 (fractional coordinates) along the b-axis. At each of the relative positions, the R-factor for data between 8.0–6.0 Å was calculated, giving rise to the plot shown in Figure 4. The translation corresponding to the lowest R-factor was applied to provide a model for rigid body refinement. This was carried out with the TNT package.[22] Three cycles of refinement against data between 8.0 and 6.0 Å lead to a drop in R-factor from 49.0% to 36.9%. Rigid body refinement was continued against data

TABLE I. Statistics of Data Collected for the Three Structures

Identifier	PEG-native	PEG-SO_4	PEG-PGH
Cell edges (Å) (*a*,*b*,*c*)	94.8, 48.3, 131.0	94.6, 48.2, 130.7	94.6, 48.0, 131.3
β-angle	100.3°	100.6°	100.3°
Maximum resolution (Å)	2.1	2.4	2.5
Observations	59,116	39,764	26,995
Overall merging R*(%)	6.3	4.8	5.7
Unique reflections	26,860	20,429	18,801
Overall completeness (%)	78.0	81.8	69.7
Final shell completeness (%)	57.6 (2.13–2.10 Å)	41.8 (2.43–2.40 Å)	47.6 (2.58–2.50 Å)

$$^{*}\text{Merging R} = \frac{\sum_h \sum_i |(\bar{I}_h - I_{h,i})|}{\sum_h \sum_i |\bar{I}_h|} * 100\%$$

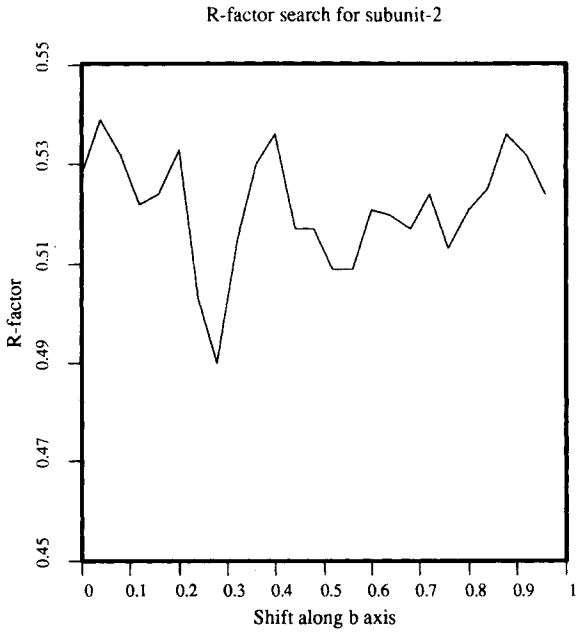

Fig. 4. R-factor search for the relative *b*- coordinate of molecule-2 with respect to molecule-1. After application of the appropriate rotations (from ALMN), and translations in the *ac*-plane (TFSGEN), molecule-1 was held in a fixed location, and molecule-2 was moved in steps of 0.04 (fractional cell lengths, corresponding to ~ 2 Å) along the *b*-axis. At each relative position, the R-factor for data between 8.0 Å and 6.0 Å was calculated (TNT package). The lowest value (49.0%) occurred at a relative translation of 0.28.

between 6.0 and 4.0 Å, at which resolution the R-factor dropped from 29.9% to 29.4% during five cycles.

Structure Refinement

Refinement of the atomic models was begun after deletion of the conformationally variable loops 6 and 7 (residue 167 to 180 and 211 to 214, respectively) from each of the two monomers. Refinement was pursued with a mixture of molecular dynamics X-ray refinement (XPLOR package[23]), and conventional positional and thermal factor refinement (TNT). The XPLOR simulated annealing protocol here employed is summarized in Table II. Between refinement cycles, manual rebuilding was performed in 2Fo-Fc SIGMAA weighted maps[24] using FRODO[25] running on an ESV10 workstation. During manual rebuilding, the residues of the flexible loops of the two monomers were gradually added back as a suitable chain tracing became visible in the electron density. Water residues were added to the structure using an automatic peak search and environment screening procedure. In this procedure, peaks larger than 3 standard deviations above the mean in an Fo-Fc map were chosen as possible water positions. These potential sites were accepted if they were found to have a potential hydrogen bonding partner (O or N atom) between 2.3 and 3.3 Å distance, and no carbon or sulphur atom within 3.2 Å. The final statistics of the refined model (PEG-native) are given in Table III.

Soaking With 0.4 M Ammonium Sulphate

A crystal grown as above was transferred to a fresh mother liquor consisting of 200 mM Tris/HCl, pH 8.8 (as measured) and 1 mM DTT, EDTA, NaN_3, and 400 mM ammonium sulphate. A higher concentration of sulphate was found to lead to dissolution of crystals grown under these conditions. The crystal was soaked for a period of one day, during which it was once transferred to a fresh soaking solution. After this period, the crystal was mounted in a siliconized quartz capillary, and used to collect a three-dimensional dataset to a resolution of 2.4 Å using the equipment and software described above. Statistics of the resulting dataset are given in Table I.

This dataset was used in rigid body refinement using the TNT package, taking as start coordinates the PEG-native structure described above. After rigid body refinement, loops 6 and 7 of each molecule were deleted, and the resulting trimmed models were used to phase SIGMAA weighted Fo-Fc and 2Fo-Fc electron density maps. The fit of the model against these maps was optimized interactively using the

TABLE II. Details of the XPLOR Simulated Annealing Protocol Employed

Nonbonded parameters	Dielectric constant = 1, maximum distance = 7.0 Å, switching function: 6.0 Å–6.5 Å, full atomic charges set to zero (Lys, Arg, Glu, Asp)
Relax stage	
Tolerance	0.05 Å
VDW repulsion turned on*	50 cycles
VDW repulsion turned off	50 cycles
Annealing stage	
Initial temperature	1,500 K
Temperature step	−25 K
Cycles at each step	25
Tolerance	0.2 Å
Final temperature	300 K
Regularization stage	100 steps of conjugate gradient refinement

*VDW = van der Waals.

program FRODO[25] running on an ESV10 workstation. Models for loops 6, and loop 7 were rebuilt into their appropriate difference electron density. Refinement of this structure was performed using a combination of conventional least squares refinement (TNT), molecular dynamics X-ray refinement (XPLOR), and interactive model building. Final statistics for the refined models are given in Table III.

Soaking With Phosphoglycolohydroxamate

PGH (Fig. 3) is a competitive inhibitor of the action of TIM, with a K_i of 4 μM.[26] Soaking of PEG-native crystals in solutions with a PGH concentration as low as 16 μM lead to crystal cracking, and prevented data collection. This problem was solved by performing the soaking experiment in a solution containing not 18% PEG6000, but rather 44% PEG6000. This is the same buffer as has been used in soaking experiments involving the 2.4MAS crystals.[27] In such a stabilization buffer, crystals could be soaked in PGH concentrations of up to 40 μM, without causing visible damage. One such crystal was mounted in a quartz X-ray capillary and used to collect a three-dimensional dataset to a resolution of 2.5 Å, using similar conditions to those described above.

Refinement of this structure was started from the PEG-native structure, after deletion of loop-6 and loop-7 from each molecule. In the first SIGMAA weighted difference map, it was apparent that PGH had bound in the active sites of molecule-2, inducing a closed loop conformation. No evidence was apparent for the binding of PGH at the active sites of molecule-1. The ligand was left out of the refinement, but the flexible loop of molecule-2 was built into the closed conformation, and a rebuild of loop-7 was performed. The protein model was then refined using a combination of molecular dynamics X-ray refinement (XPLOR), and conventional positional refinement (TNT). When the R-factor had reached 19% (15.0–2.5 Å), further maps were calculated. PGH was built into its corresponding density, and a number of water molecules were added, using the protocol described above. Further refinement was performed using only the TNT package, and included restrained individual atomic thermal parameter refinement. The geometry of PGH used in this refinement was taken from an energy minimized model of PGH generated by the BIOGRAF package.[28] Final refinement statistics of the model are given in Table III.

For the purposes of analysis, models were superimposed on the basis of 105 CA positions forming the eight α-helices and 8 β-strands.

RESULTS

Criteria of Model Quality

The structure of trypanosomal TIM has been solved in the monoclinic space group *C*2. Crystals of trypanosomal TIM in this space group diffract beyond 2.1 Å. The refinement statistics presented in Table III for the PEG-native structure indicate a well refined structure. In addition, Figure 5 shows that the phi/psi combinations observed in this new structure are near acceptable regions of the Ramachandran plot. The only two seriously deviating residues are the catalytic lysines (Lys13) from each of the two molecules. These are seen in all TIM structures to occupy similar conformations, with positive phi and negative psi values. This conformation is presumably required to allow an optimal active site architecture.

In Figure 6 is presented the main chain real space density correlation coefficient for monomers from each molecule as a function of residue number. This plot shows the mean correlation for main chain atoms of each residue between 2Fo–Fc α_{calc} electron density, and electron density calculated directly from the atomic parameters. For the whole sequence, the correlation is above 0.75. Generally the correlation is considerably higher (average value = 0.86), except in the region of the flexible loop of molecule-2 (dotted line, residues 167–180). This flexible part of the structure is free from crystal contacts in molecule-2, whereas it is involved in such contacts in molecule-1. Nevertheless, the interpretation of the electron density in this region is correct, as shown from the fit of the flexible loop into omit electron density after omit refinement done after completion of the structure refinement (Fig. 7).

The Structure of Trypanosomal TIM in the New Crystal Form

In the PEG-native structure, the presence of 50 mM ammonium sulphate in the crystallization medium has not given rise to a sulphate molecule

TABLE III. Statistics of the Refinement of the Three Structures

Model	PEG-native	PEG-SO4	PEG-PGH
Protein atoms	3,778	3,778	3,778
Water atoms	200	81	61
Ligand atoms		10 (sulphate)	10 (PGH)
Crystallographic parameters			
Resolution (Å)	2.1	2.4	2.5
Reflections in refinement	26,879	18,719	14,229
R-factor* (%)	17.6	15.8	14.7
Geometric parameters†			
rms bond length deviation (Å)	0.016	0.020	0.014
rms bond angle deviation (degrees)	2.46	2.51	2.50
$\chi^1\chi^2$ imperfection (degrees)‡	27.9	31.6	35.7
rms delta B for bonded atoms (Å^2)	7.2	12.0	8.1

* $$\text{R-factor} = \frac{\sum_h |(F_{obs,h} - F_{calc,h})|}{\sum_h |F_{obs,h}|} * 100\%,$$

calculated by TNT with modified scaling to model bulk solvent. Low resolution limit = 15 Å.

†Unless otherwise stated, calculated with the TNT refinement package.

‡Rms deviation from Ponder and Richards side chain torsion angle database,[30] as calculated by the program TORSIONS (Noble, M.E.M., unpublished results).

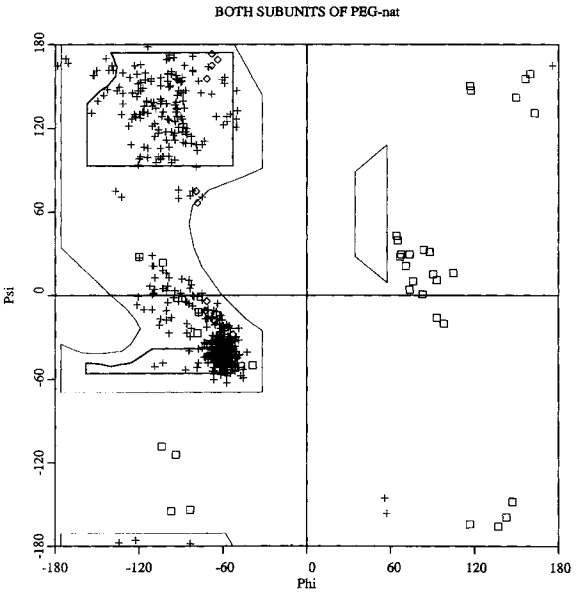

Fig. 5. Ramachandran plot of the refined PEG-native model. The scatter of phi-psi combinations observed in molecule-1 and molecule-2 is depicted. Thick lines surround the fully allowed regions,[34] and the thin lines surround regions allowed with a relaxed van der Waals constraint. Plusses are used for the values observed, except in the case of prolines (diamonds), and glycines (squares).

bound at the active site of either molecule. Both flexible loops are seen to occupy the open conformation, consistent with other structures of ligand-free TIM. The temperature factor profiles of the two molecules are presented in Figure 8. Molecule-1 has a lower mean B-factor for main chain atoms than does molecule-2 (15.4 Å^2, compared to 20.4 Å^2), and this difference is most marked in the region of the flexible loop. This is correlated with the presence of lattice contacts involving the flexible loop of molecule-1, which do not occur for the flexible loop of molecule-2. A comparison of the open loop structures observed in each of the two molecules with that observed in subunit-1 of the 2.4MAS structure shows that for each residue the rms displacement, as calculated from the four main chain atoms, is less than 1 Å, despite the fact that in molecule-1 loop-6 is stabilized by crystal contacts, whereas in molecule-2 it is not, causing high mobility (Fig. 8).

The Structure of Trypanosomal TIM in the New Crystal Form in the Presence of 0.4 M Ammonium Sulphate

The structure of this new crystal form after soaking with 0.4 M ammonium sulphate has also successfully been determined (termed PEG-SO4). This soaking could be performed on the crystals without transfer to a "stabilization buffer" containing a higher PEG6000 concentration to that in which the crystal was grown. Higher concentrations of sulphate (for example 0.8 M), caused crystals to dissolve under these conditions. In these crystals, a sulphate molecule can clearly be seen to bind to the active site of molecule-2, as seen from a difference map calculated using phases from the PEG-native structure, and data from the PEG-SO4 crystal (Fig. 9). This sulphate position appeared as the highest peak in such a map (height more than 8 σ). The average atomic B-factor of a sulphate molecule refined in this electron density is high (92 Å^2, compared to a mean main chain B-factor of 24.8 Å^2). The possibility that this peak might represent a water molecule was discounted for two reasons: firstly, a

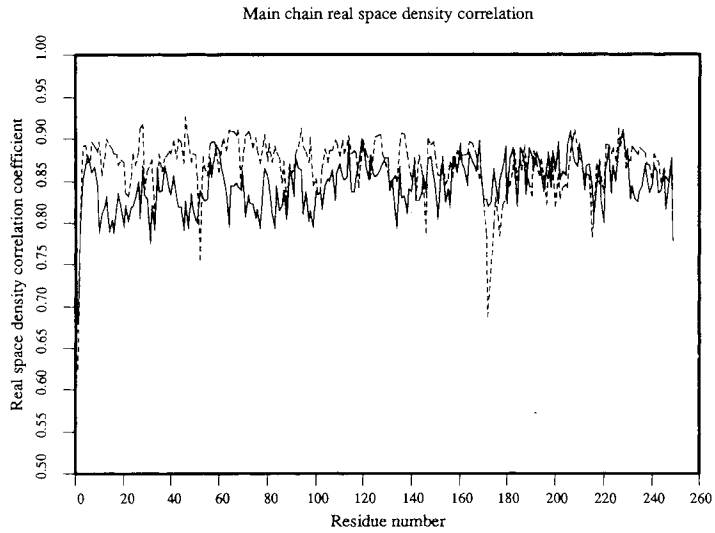

Fig. 6. Real space density correlation coefficient as a function of residue number. The mean real space density correlation coefficient for main chain atoms of molecule-1 (solid line), and molecule-2 (broken line) is plotted as a function of residue number. The values were calculated using the program O, with the observed map being a SIGMAA weighted 2Fo-Fc α_{calc} electron density map from the final refined structure.

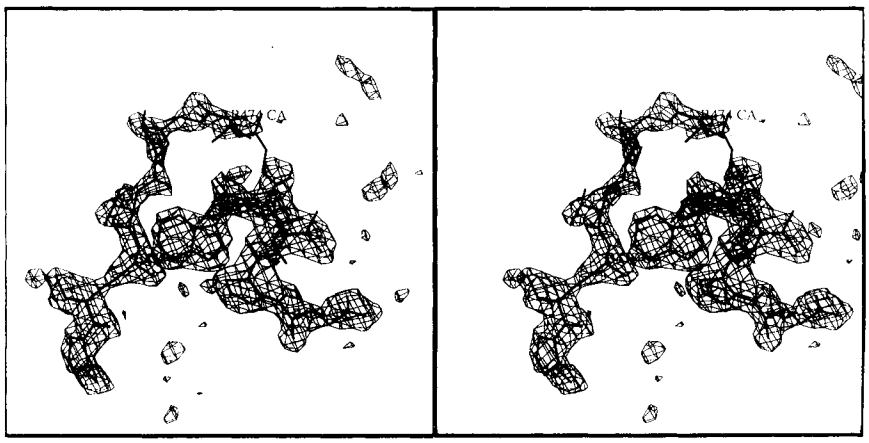

Fig. 7. Stereograhic picture of the fit of loop-6 of molecule-2 into omit electron density. After completion of the refinement of the PEG-native structure, residues 167–180 of molecule-2 were deleted, and the model was subjected to 5 cycles of joint positional and thermal factor refinement using the conjugate direction method of the TNT package. The resulting model was used to calculate phases and Fcs for an Fo-Fc α_{calc} map calculation. The map is contoured at a level of 3 standard deviations.

water molecule placed in this position is too far from any protein atom to form hydrogen bonds (shortest distance to protein atoms = 3.9 Å), and secondly, there is no strong electron density peak for a water molecule at this position in the PEG-native structure. A similarly positioned peak appears in the active site of molecule-1. This peak is considerably weaker, having a ranking of eight in the original list of difference electron density peaks.

The position of the sulphate in this structure is close, but not identical, to that observed for the sulphate molecule in the active site of molecule-2 of the 2.4MAS structure; the sulphur atom in the PEG-SO4 structure is displaced by about 1.0 Å relative to that of the 2.4MAS structure, lying slightly further out of the active site (see also Fig. 13). After structure superposition on the basis of the 8 α-helices and 8 β-strands, the sulphate positioned in this structure is within 0.2 Å of the sulphate position in native crystals of chicken TIM. In the PEG-SO4 structure, the orientation of the sulphate molecule cannot be defined exactly on the basis of the electron density, consistent with the high atomic B-factors of the ligand. The contacts made by the sulphate atoms are therefore hard to determine accurately. The sulphate ion is hydrogen-bonded to some water molecules but

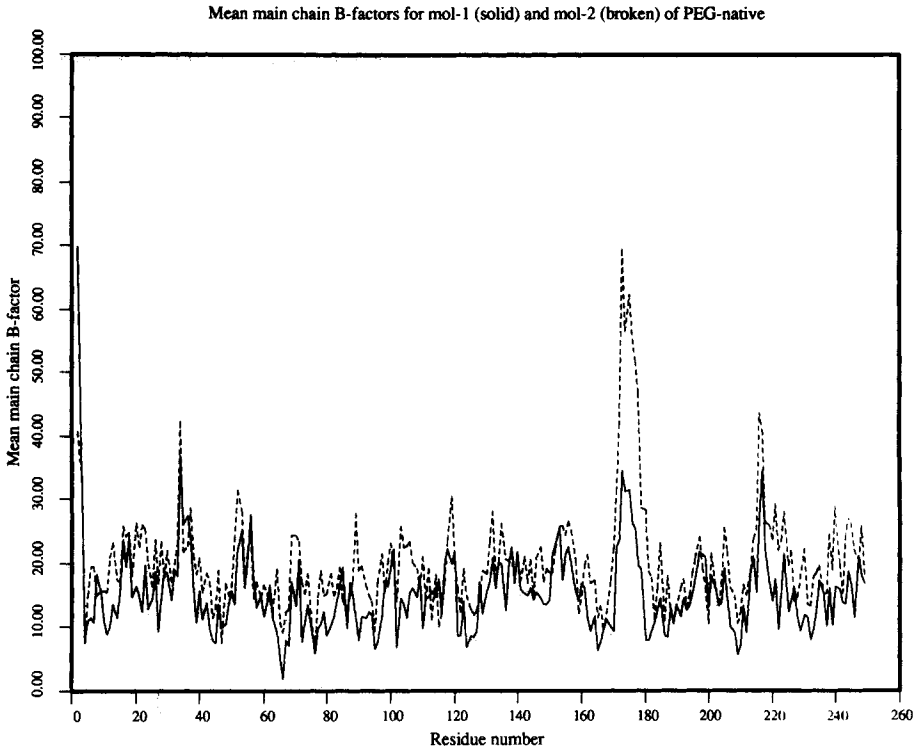

Fig. 8. Temperature factor profile of the PEG-native structure. The mean main chain temperature factors of residues of molecule-1 (solid line), and molecule-2 (broken line) are shown as a function of residue number.

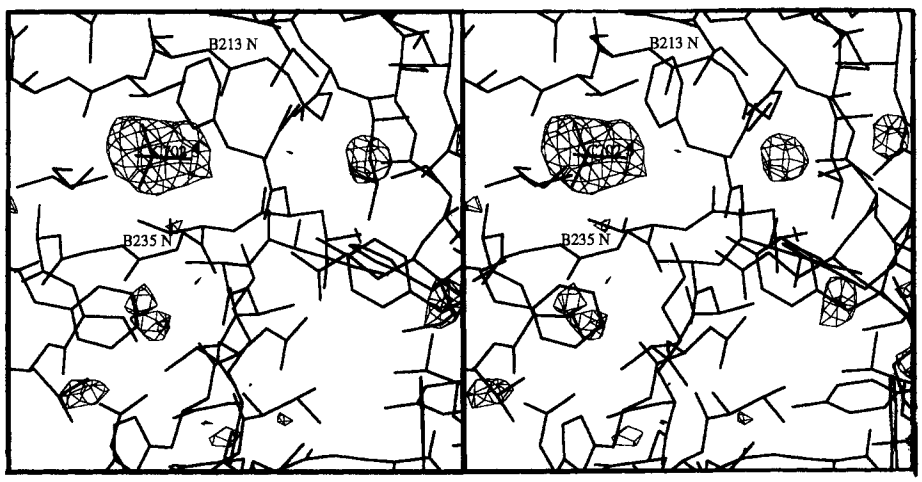

Fig. 9. Stereo picture of difference electron density for the sulphate in molecule-2 of the PEG-SO4 structure. Fo-Fc α_{calc} electron density with data from the PEG-SO4 dataset, and Fc, and phases from the PEG-native structure is contoured at 4σ, and drawn in thin lines. The atomic model is that of the refined PEG-SO4 model. Labels are present on the sulphur atom of the sulphate moiety (C702), on one of the loop-8 residues responsible for coordinating the sulphate (B235), and on the loop-7 residue Ser213 (B213). The labeled nitrogen atom of this last residue is in a different conformation in other TIM-ligand complexes, to allow it to hydrogen bond with a phosphate or sulphate group.

it is probably held in place via hydrogen bonds between the sulfate oxygen atoms and the OG(Ser213) of loop-7 as well as N(Gly234) and N(Gly235) of loop-8. The sulphate in the PEG-SO4 structure does not form a hydrogen bond with the flexible loop, since the flexible loops in both molecules of this structure are in the open conformation. A further determinant of the interactions of the sulphate moiety with the protein is the conformation of loop-7 (Tyr210 Gly211 Gly212 Ser213). In the 2.4MAS structure, this loop shows structural heterogeneity,[3] with alternate structures interconverting through

the flipping of the peptide plane Gly212-Ser213. In one of the possible orientations, which is preferred in the 2.4MAS structure, the peptide nitrogen of Ser213 is able to hydrogen-bond to the sulphate group, whilst in the other, a short contact would be formed between an oxygen of the sulphate group and the peptide oxygen of Gly212. In the PEG-SO4 structure, loop-7 appears to adopt the latter of these two conformations. This conformation is the same as that observed in the PEG-native structure. In Figure 13, the three positions of sulphate (PEG-SO4), sulphate (2.4MAS) and PGH (PEG-PGH) are compared together with the three associated structures of loop-6 and loop-7.

The Structure of Trypanosomal TIM in the New Crystal Form in the Presence of 40 μM PGH

In order to bind phosphoglycolohydroxamate to the new crystal form without disrupting the crystals, it was necessary first to transfer the crystals to a buffer containing a higher concentration (44%) of PEG6000 to that used in the inital crystallization experiment (18%). An Fo-Fc difference fourier using the PEG-native structure and the PEG-PGH data revealed that PGH was bound only at the active site of molecule-2, i.e., that molecule in which the flexible loop is free from crystal contacts. Correlated with the binding of PGH, the flexible loop was seen to have adopted the closed conformation, and loop-7 was seen to adopt the conformation it occupies in structures of other TIM substrate analogue complexes. Direct hydrogen bonds to the phosphate group are formed exclusively by peptide nitrogens from loops 8, 7, and 6: Gly234 and Gly235 (from loop-8) are hydrogen-bonded to O3P and O1P respectively, while Ser213 (from loop-7) forms a hydrogen bond to O2P and O3P, and Gly173 (from loop-6) to O2P.

The hydroxamate group of PGH is coordinated by hydrogen bonds from NE2 of His95 (to O5 and O6), and ND2 of Asn11 (to O6). There is also a hydrogen bond between the catalytic glutamate residue (Glu167) and O6, and a longer interaction occurs between NZ of Lys 13, and O5 (3.9 Å). The full list of protein ligand contacts shorter than 3.5 Å is given in Table IV. Figure 10 shows the symmetrical disposition of hydrogen bonding groups about the hydroxamate function. The catalytic glutamate has adopted its characteristic swung-in conformation, with one carboxyl oxygen poised over N1. This nitrogen is analogous to carbon atom C3 (Fig. 3) of the substrate DHAP, from which abstraction of a proton occurs at the start of the reaction cycle. This nitrogen position is also close to the position of a conserved water molecule in unliganded structures.[29] After superimposing this structure for trypanosomal TIM complexed with PGH upon that of yeast TIM complexed with PGH,[11] an rms coordinate difference of 0.3 Å is observed for all PGH atoms. Such a good agreement is remarkable for independently produced structures, given that the source of the enzyme is different in the two cases (with a sequence identity of 49%), and that the trypanosomal TIM complex, produced by soaking rather than cocrystallization, is deduced from a somewhat incomplete lower resolution dataset.

TABLE IV. Contacts Less Than 3.5 Å Between Trypanosomal TIM and PGH

Polar-polar contacts			Other contacts	
Ligand atom	Distance (Å)	Protein atom	Distance (Å)	Protein atom
O1P	3.0	N Gly235		
O2P	2.9	N Ser213		
	3.0	N Gly173		
O3P	3.1	N Gly234		
	3.4	N Ser213		
O4P*	3.2	N Gly234	3.3	CA Gly234
C1			3.3	N Gly234
C2			3.2	OE2 Glu167
O5	2.7	NE2 His95		
N1	2.4	OE2 Glu167	3.3	CD Glu167
	3.4	OE1 Glu167	3.3	CG Glu167
	3.4	O Leu232		
O6	2.9	OE2 Glu167	3.1	CG Leu232
	3.1	OE1 Glu167	3.1	CD2 Leu232
	3.5	NE2 His95	3.4	CD2 His95
	3.5	ND2 Asn11	3.4	CD Glu167

*O4P is between P and C1 (see Fig. 3).

Conformational Changes Upon Ligand Binding

A coordinate comparison of molecule-2 of the PEG-PGH structure with the PEG-native structure is shown in Figure 11. Changes in conformation are apparent for loops 5–7. These changes are very similar in extent and nature to the differences observed between the open and closed loop states of the 2.4MAS crystal form (also shown in Fig. 11). Loop-6 has undergone a shift of maximally 7 Å to form a direct hydrogen bond from the peptide nitrogen of Gly173 to the phosphate group of the transition-state analogue. Loop-7 has undergone a peptide flip which allows a hydrogen bond from the peptide nitrogen of Ser-213 to the phosphate group of PGH.

The shift of loop-5 can be related to a change in a hydrogen bonding network which results from the closure of loop-6 over the active site. In this network, the completely conserved residue Glu129 plays a key role (Fig. 12). In the open state, Glu129 interacts via OE2 with OH of Tyr166, which in turn forms a direct hydrogen bond to NE1 of the flexible loop residue Trp170. OE1 of Glu129 is free to interact with the loop 5 residue Arg134 in the short helix

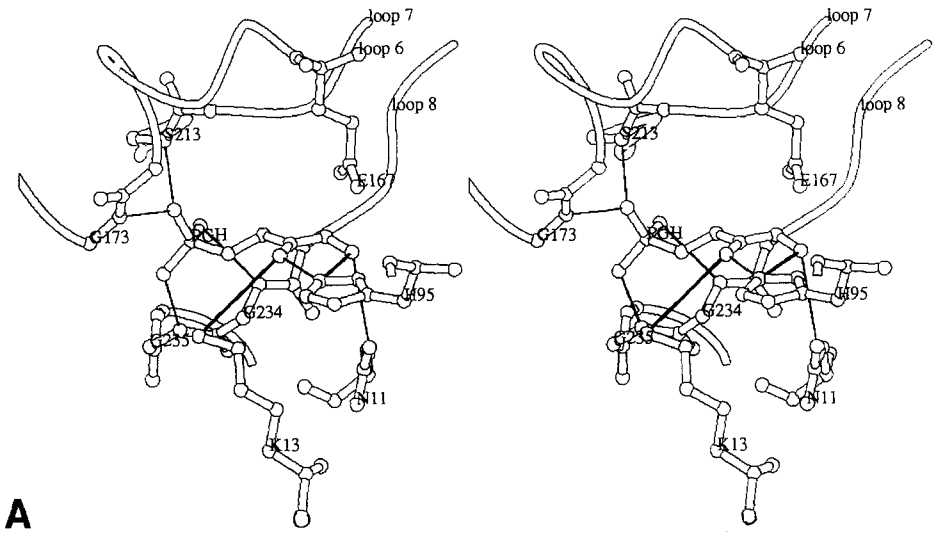

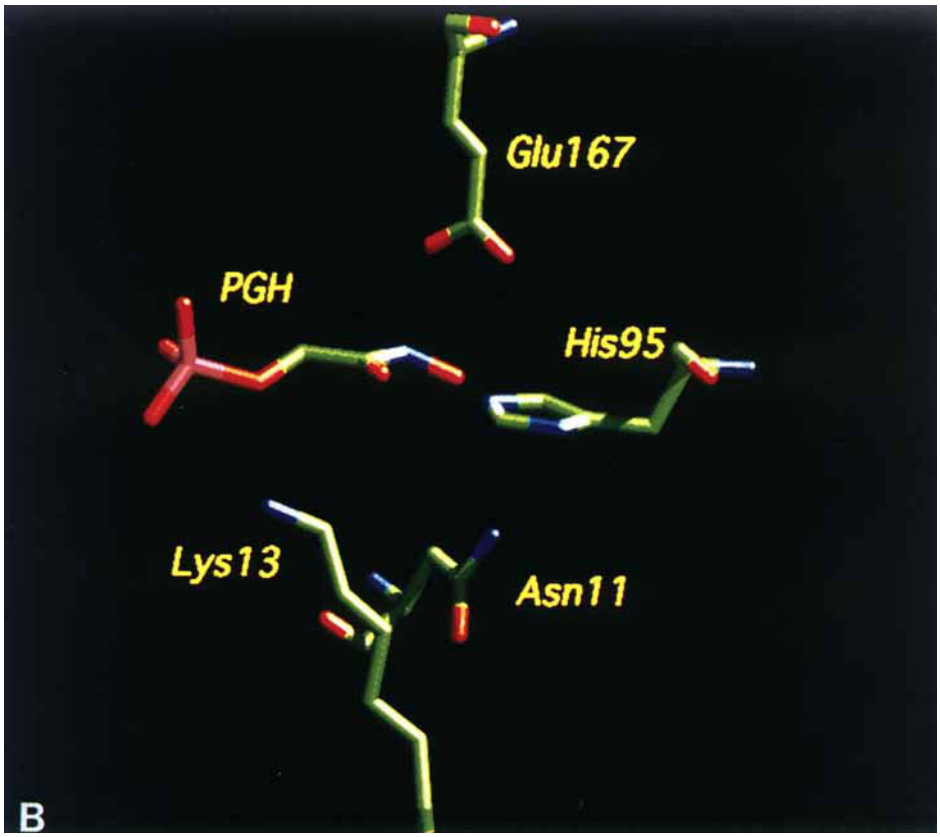

Fig. 10. **A:** Coordination of the PGH molecule in molecule-2 of the PEG-PGH structure. The side chains of the catalytic residues Asn11, Lys13, His95, and Glu167 are shown. Some hydrogen bonds are emphasized by a black line. **B:** Schematic view of the relationship between PGH and the catalytic residues mentioned above. This figure was made with the program XRENDER (M.N., unpublished).

in loop-5 (2.9 Å to NE, and 2.8 Å to NH1), and with Thr139 (2.9 Å to OG1) at the end of this short helix and the beginning of helix 5. In the closed state, Trp170 has moved somewhat further away from Tyr166, and a direct hydrogen bond between OH (Tyr166) and NE1 (Trp170) is no longer possible.[29] Instead, the carboxylate group of Glu129 sits between Tyr166 and Trp 170, due to a change in its χ^3

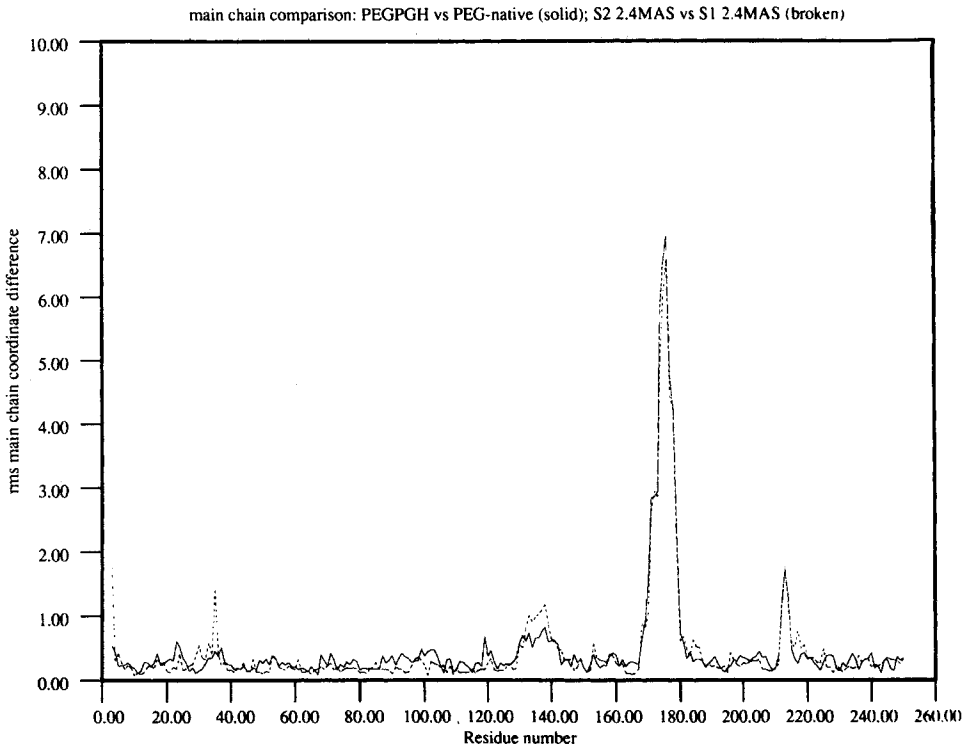

Fig. 11. Conformational changes on ligand binding. The rms main chain coordinate difference after superposition for the comparison between molecule-2 PEG-PGH and molecule-2 PEG-native is shown in the solid line. The equivalent comparison, between subunit-1 2.4MAS and subunit-2 2.4MAS is shown in the broken line. Common regions of difference lie in the regions of loop-5 (129–139), loop-6 (167–180), and loop-7 (210–214).

angle, and a small rigid body shift of loop-5. The change in conformation of Glu129 breaks the hydrogen bond from OE2 to OG1 of Thr139 (distance now 3.9 Å), but causes shorter hydrogen bonds from OE2 to NE and NH1 of Arg134. The side chain torsion angle combination of Glu129 in either conformation is $\chi^1(\approx 82)$ and $\chi^2(\approx -70)$. This combination lies in the least occupied family of χ^1/χ^2 combinations for glutamate residues according to the analysis of Ponder and Richards.[30] In the closed form, OG1 of Thr139 has no protein hydrogen-bonding partner. Thus, the effects of the closure of the flexible loop are propagated along the loop-5 helix through changes in side chain interactions.

DISCUSSION

The agreement between the ligand-free structure of trypanosomal TIM determined in two different space groups is rather good. For molecule-2 of the PEG-native structure compared to subunit-1 of the 2.4MAS structure, main chain atoms agree to within 0.30 Å rms, and for all atoms with B factors less than 35 $Å^2$, the rms agreement is 0.33 Å (for 1,600 atoms out of 1,889 in a subunit). The coordinate difference which exists is comprised of error in each of the two sets of coordinates, and genuine differences in structure due to differences in crystal packing and the mother liquor in which the crystals are grown. Neither of these two components can, therefore, be very large.

It is interesting to note, therefore, that the sulphate binding properties of typanosomal TIM in this new space group are somewhat different. These differences cannot be due to a difference in protonation state of the sulphate ion, as the pH (7.0 (2.4MAS) and 8.8 (PEG-PGH)) assures that the sulphate ion occurs as SO_4^{2-} in both experiments. Whereas in the 2.4MAS crystal form, binding of a sulphate ion at the active site is accompanied by closure of the flexible loop, in the PEG-SO4 crystal form there is no closure of the flexible loop over the active site to which a sulphate molecule is clearly bound. This is consistent with the structure of the flexible loop in crystals of chicken TIM grown from ammonium sulphate, which also have sulphate moieties bound at each of the active sites, but have open flexible loops. It would, however, be incorrect to deduce that the 2.4MAS trypanosomal TIM crystals are constrained to have a closed flexible loop structure by crystal contacts, since in other experiments, it has been shown that diffusion of sulphate away from the active site allows the flexible loop to adopt an open conformation.[12] Notably, the position of the sulphate ion in the new trypanosomal crystal form,

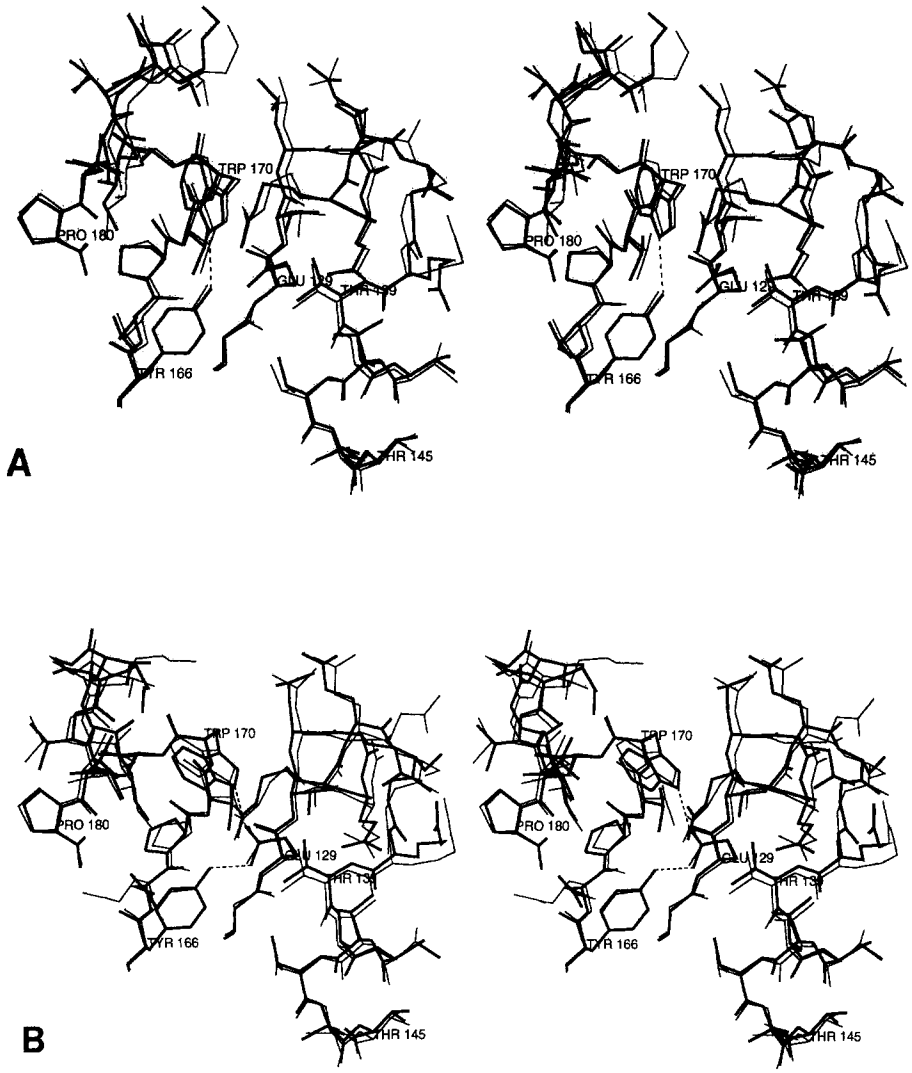

Fig. 12. The conformational change affecting the short helix in loop-5 between residues Glu129 and Thr139. **A:** Two "open" structure of trypanosomal TIM: Subunit-1 of the 2.4MAS structure, and molecule-2 of the PEG-native structure. The dotted line indicates the hydrogen bond (3.0 Å) between OH (Tyr166), NE (Trp170). **B:** Two "closed" structure of trypanosomal TIM: Subunit-2 of the 2.4MAS structure, and molecule-2 in the PEG-PGH structure. The dotted lines indicate the hydrogen bonds, 2.6 Å and 2.3 Å, between OH (Tyr166), OE2 (Glu129), and OE1 (Glu129), NE (Trp170) respectively; the distance between OH (Tyr166), NE (Trp170) is 4.8 Å.

where the flexible loop is open, resembles much more closely the position of sulphate in chicken TIM crystals than its position in subunit-2 of the 2.4MAS structure. Apparently sulphate has the property of being able to partially stablise a closed flexible loop conformation, but this conformation is also dependent on other details of the protein structure which may be influenced by crystal packing or a combination of differences in crystal packing and mother liquor. In this respect, it is important to note that loop-6 of subunit-2 of 2.4MAS crystals, from which sulphate is diffused out, adopts an open conformation,[12] but it appears that no coordinated movement of loop-5 can occur. Instead, this loop maintains the conformation it has in ligand-bound structures. This observation has been discussed elsewhere.[31]

The constituent monomers of each dimer in the new crystal form are crystallographically, and therefore exactly, identical, both in the open and in the closed conformation. This contrasts with the 2.4MAS structure, where subunit-1 has an open conformation, and subunit-2 has an almost closed conformation. The *C*2 open conformation is identical to subunit-1 of the 2.4MAS structure, and the *C*2 closed conformation is identical to subunit-2 of the 2.4MAS structure when substrate analogues are bound to the active site of this molecule (Figs. 11, 12). This is further evidence that the two active sites have identical properties, and function independently.

The PEG-PGH structure confirms the genuine nature of a change in loop-5 conformation and hydro-

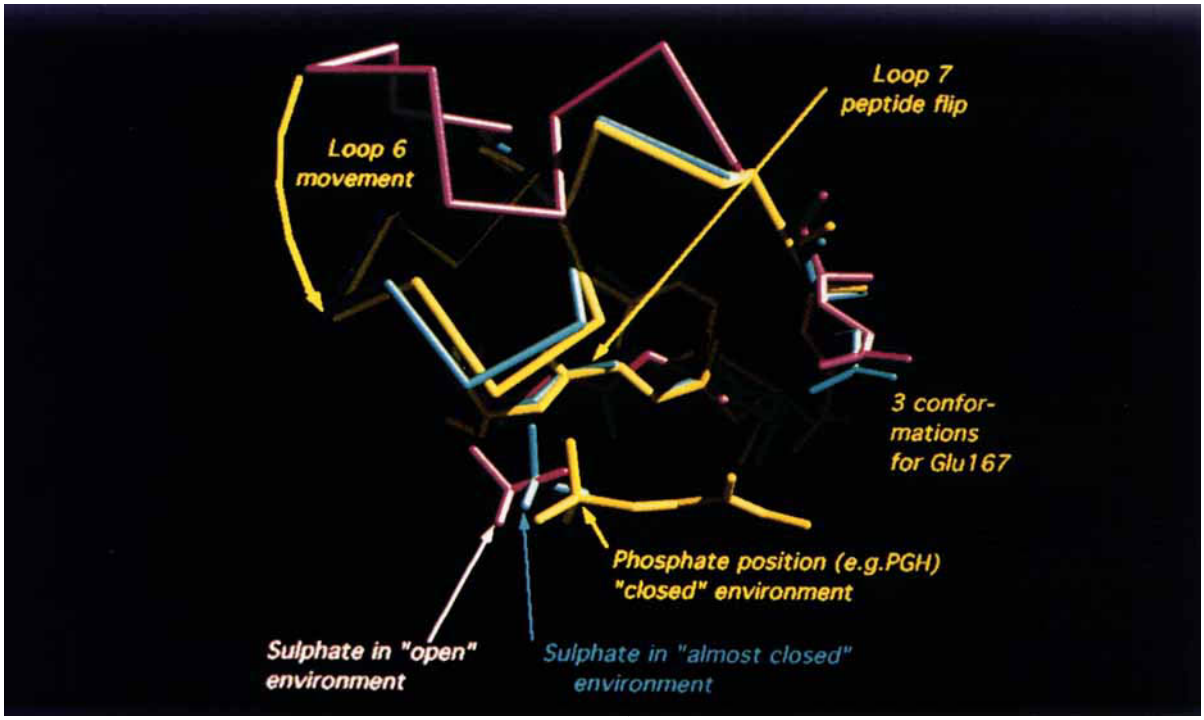

Fig. 13. Three different structures can be seen in this drawing: sulphate bound in the "open" state (red), sulphate bound in the "almost closed" state (blue;[3]), and PGH bound to the "closed" state (yellow). Glu167 is the first residue of loop-6, and Cα atoms of loop-6 residues 168–180 are also shown. Residues Tyr210-Gly211-Gly212-Ser213 of loop-7 are depicted as well. The loop-7 peptide flip affects the position of the peptide oxygen of Gly212. See text for further details.

gen bonding pattern on the switch from the open to the closed state. The shift of the short helix in loop-5 is observed in this new crystal form as a difference between the PEG-native structure, and the PEG-PGH structure. That this movement is also observed in a new crystal form, independent of crystal packing, confirms its relevance in the catalytic mechanism. The changes in the hydrogen bonding in this region of the protein, between two clearly defined hydrogen bonding networks, could be part of a mechanism which makes the conformational changes in TIM into an essentially two-state process.

Another loop rearrangement which is seen to occur also in the new crystal form is that of loop-7. The flip of the peptide bond Gly212-Ser213, which occurs in loop-7 upon ligand binding, causes the ϕ/ψ combination of Ser213 to change from (−83,118) to (47,51) in the closed state. This transition requires the crossing of a nonallowed region of Ramachandran space, and so might be thought to introduce an energy barrier to ligand binding. Model calculations[32] suggest that this energy barrier could be as much as 10 kcal.mol^{-1}. The magnitude of this energy barrier will, however, be modulated by the fact that the conformation prior to ligand binding is not an energetically favourable one. This is because the peptide nitrogen of residue Gly212 does not have a classical hydrogen bonding partner, but rather points to the aromatic ring of Tyr210.[3] This conformation, observed in open structures, would still be preferable to the loop conformation observed in closed structures, but in liganded closed structures, the active site ligand provides a hydrogen-bonding partner to the peptide nitrogen of Ser213. Without an active site ligand, this peptide nitrogen would not have a hydrogen bonding partner in the closed loop conformation. The peptide flip of residue Gly212 is essential for allowing the phosphate to bind in its observed position, as it replaces an unfavorable interaction of O(Gly212)-O3P(PGH), 3.7 Å (in the hypothetical open structure with bound PGH), by favorable interactions between N(Ser213)-O2P(PGH), 2.9 Å and N(Ser213)-O3P, 3.4 Å, as observed in the PEG-PGH structure (Fig. 10). It is tempting to speculate that the peptide flip and the associated conformational change of loop-7 synchronizes the binding of ligand with the closing of loop-6, because in the closed loop-7 conformation OG(Ser213) has moved outwards 1.1 Å and stabilizes the closed loop-6 conformation via hydrogen bonds between OG(Ser213)-O(Ala271), 2.6 Å, and OG(Ser213)-N(Gly275), 3.4 Å.

In isotope-labeled isomerization reactions catalyzed by TIM, it is found that only 3–4% of the protons abstracted from carbon atoms of the substrate go on to be found on carbon atoms of the product.[5] The remaining 96–97% of these protons exchange

with protons of the bulk solvent. In pulse chase experiments using tritium-labeled enzyme, Rose has provided evidence that in the cases where the product carbon carries a proton from the bulk solvent, it has acquired this proton via a proton exchanging group of the protein ("internal" exchange).[33] Glu167, which performs the role of the catalytic base, occupies a well defined "swung-in" conformation in the TIM-PGH complexes, and by analogy in the TIM substrate complex. From the available high resolution structures, such as the yeast TIM-PGH complex[11] and the trypanosomal TIM glycerol-3-phosphate complex,[3] it can be deduced that the proton bound to OE1, OE2 (Glu167) can, in principle, be exchanged via a water molecule which is bound in these complexes near OE1. As far as "internal" exchange is concerned, the only nearby protein groups, in PEG-PGH and in the yeast TIM-PGH complex, able to perform proton exchange and within 4 Å of OE1, OE2 (Glu167) are NE2 (His95) and SG (Cys126). This suggests that these atoms could be involved in this "internal" proton exchange.

ACKNOWLEDGMENTS

We acknowledge Dr. Fred Opperdoes and Dr. Paul Michels for their drive towards producing large quantities of recombinant trypanosomal TIM, and Dr. Kathryn Pratt who was responsible for producing a successful overexpression system. Phosphoglycolohydroxamate was kindly given to us by Prof. Jeremy Knowles. Dr. P. Artymiuk provided us with coordinates of the refined structure of chicken TIM, and Dr. R.C. Davenport provided us with the structure of the yeast TIM-PGH complex for comparative purposes. This work was funded in part by EC grant BIOT-CT90-0182 to R.K.W. We are also indebted to Dr. Paul Tucker for his help with the data collection facilities at the EMBL in Heidelberg. Finally, we would like to thank Prof. Wim Hol and Dr. Christophe Verlinde for many interesting discussions about ligand binding in TIM. We have appreciated the comments of the referees. The coordinates of the PEG-PGH have been submitted to the Brookhaven Protein Data Bank (ITRD).

REFERENCES

1. Banner, D.W., Bloomer, A.C., Petsko, G.A., Phillips, D.C., Pogson, C.I., Wilson, I.A., Corran, P.H., Furth, A.J., Milman, J.D., Offord, R.E., Priddle, J.D., Waley, S.G. Structure of chicken muscle triosephosphate isomerase at 2.5 angstrom resolution using amino acid sequence data. Nature 255:609–614, 1975.
2. Lolis, E., Alber, T., Davenport, R.C., Rose, D., Hartman, F.C., Petsko, G.A. Structure of yeast triosephosphate isomerase at 1.9-Å resolution. Biochemistry. 29:6609–6618, 1990.
3. Wierenga, R.K., Noble, M.E.M., Vriend, G., Nauche, S., Hol, W.G.J. Refined 1.83Å structure of trypanosomal triosephosphate isomerase crystallized in the presence of 2.4M ammonium sulphate. A comparison with the structure of the trypanosomal triosephosphate isomerase-glycerol-3-phosphate complex. J. Mol. Biol. 220:995–1015, 1991.
4. Brändén, C-I. The TIM barrel–the most frequently occurring folding motif in proteins. Curr. Opin. Struct. Biol. 1:978–983, 1991.
5. Knowles, J.R., Albery, W.J. Perfection in enzyme catalysis: The energetics of triosephosphate isomerase. Accts. Chem. Res. 10:105–111, 1977.
6. Alber, T., Banner, D.W., Bloomer, A.C., Petsko, G.A., Phillips, S.D.C., Rivers, P.S., Wilson, I.A. On the three dimensional structure and catalytic mechanism of triosephosphate isomerase. Phil. Trans. Roy. Soc Lond. Ser. B. 293:159–171, 1981.
7. Noble, M.E.M., Wierenga, R.K., Lambeir, A.-M., Opperdoes, F.R., Thunnissen, A.-M.W.H., Kalk, K.H., Groendijk, H., Hol, W.G.J. The adaptability of the active site of trypanosomal triosephosphate isomerase as observed in the structures of three different complexes. Proteins 10:50–69, 1991.
8. Verlinde, C.L.M.J., Noble, M.E.M., Kalk, K.H., Groendijk, H., W., R.K., Hol, W.G.J. Anion binding at the active site of trypanosomal triosephosphate isomerase: Monohydrogen phosphate does not mimic sulphate. Eur. J. Biochem. 198:53–57, 1991.
9. Noble, M.E.M., Verlinde, C.L.M.J., Groendijk, H., Kalk, K.H., Wierenga, R.K., Hol, W.G.J. Crystallographic and molecular modelling studies on trypanosomal triosephosphate isomerase: A critical assessment of the predicted and observed complex with 2-phosphoglycerate. J. Med. Chem. 34:2709–2718, 1991.
10. Lolis, E., Petsko, G.A. Crystallographic analysis of the complex between triosephosphate isomerase and 2-phosphoglycollate at 2.5Å resolution: Implications for catalysis. Biochemistry 29:6619–6625, 1990.
11. Davenport, R.C., Bash, P.A., Seaton, B.A., Karplus, M., Petsko, G.A., Ringe, D. Structure of the triosephosphate isomerase-phosphoglycolohydroxamate complex: An analogue of the intermediate of the reaction pathway. Biochemistry 30:5821–5826, 1991.
12. Wierenga, R.K., Noble, M.E.M., Postma, J.P.M., Groendijk, H., Kalk, K.H., Hol, W.G.J., Opperdoes, F.R. The crystal structure of the open and the closed conformation of the flexible loop of trypanosomal triosephosphate isomerase. Proteins 10:33–49, 1991.
13. Joseph, D., Petsko, G.A., Karplus, M. Anatomy of a conformational change: Hinged lid motion of the triosephosphate isomerase loop. Science 249:1425–1428, 1990.
14. Pompliano, D.L., Peyman, A., Knowles, J.R. Stabilization of a reaction intermediate as a catalytic device: Definition of the functional role of the flexible loop in triosephosphate isomerase. Biochemistry 29:3186–3194, 1990.
15. Lambeir, A.-M., Opperdoes, F.R., Wierenga, R.K. Kinetic properties of triosephosphate isomerase from Trypanosoma brucei brucei. A comparison with the rabbit muscle and yeast enzymes. Eur. J. Biochem. 168:69–74, 1987.
16. Borchert, T.V., Pratt, K., Zeelen, J.Ph., Callens, M., Noble, M.E.M., Opperdoes, F.R., Michels, P.A.M., Wierenga, R.K. Overexpression of trypanosomal triosephosphate isomerase in *Escherichia coli* and characterisation of a dimer-interface mutant. Eur. J. Biochem. 211:703–710, 1993.
17. Messerschmidt, A., Pflugrath, J.W. Crystal orientation and X-ray pattern prediction for area detector diffractometer systems in macromolecular crystallography. J. Appl. Cryst. 20:306–315, 1987.
18. Kabsch, W. Evaluation of single-crystal X-ray diffraction data from a position-sensitive detector. Acta. Cryst. Sec. A. 21:916–924, 1988.
19. Crowther, R.A. The fast rotation function. In: "The Molecular Replacement Method." Rossmann, M.G. (ed.). New York: Gordon and Breach, 1972:173–178.
20. CCP4. The S.E.R.C. (U.K.) Collaborative computing project no. 4, a suite of programs for Protein Crystallography, distributed from Daresbury Laboratory, Warrington, WA4 4AD, U.K., 1979.
21. Crowther, R.A., Blow, D.M. A method of positioning a known molecule in an unknown crystal structure. Acta. Cryst. 23:544–548, 1967.
22. Tronrud, D.E., Ten Eyck, L.F., Matthews, B.W. An efficient general-purpose least squares refinement program for macromolecular structures. Acta Cryst. Sect. A. 43: 489–501, 1987.
23. Brünger, A.T., Kuriyan, J., Karplus, M. Crystallographic

R factor refinement by molecular dynamics. Science 235: 458–460, 1987.
24. Read, R.J. Improved Fourier coefficients for maps using phases from partial structures with errors. Acta Cryst. Sect. A. 42:140–149, 1986.
25. Jones, T.A. Interactive computer graphics: FRODO. Methods Enzymol. 115:157–171, 1985.
26. Collins, K.D. An activated intermediate analogue. The use of phosphoglycolohydroxamate as a stable analogue of a transiently occurring dihydroxyacetone phosphate-derived enolate in enzymatic catalysis. J. Biol. Chem. 249: 136–142, 1974.
27. Schreuder, H.A., Groendijk, H., van der Laan, J.M., Wierenga, R.K. The transfer of protein crystals from their orignal mother liquor to a solution with a completely different precipitant. J. Appl. Cryst. 21:426–429, 1988.
28. BIOGRAF. Biodesign Inc, USA, 1989.
29. Wierenga, R.K., Borchert, T.V., Noble, M.E.M. Crystallograhic binding studies with triosephosphate isomerases: Conformational changes induced by substrate and substrate-analogues. FEBS 307:34–39, 1992.
30. Ponder, J.W., Richards, F.M. Tertiary templates for proteins. Use of packing criteria in the enumeration of allowed sequences for different structural classes. J. Mol. Biol. 193:775–791, 1987.
31. Wierenga, R.K., Noble, M.E.M., Davenport, R.C. Comparison of the refined crystal structures of liganded and unliganded chicken, yeast, and trypanosomal triosephosphate isomerase. J. Mol. Biol. 224:1115–1126, 1992.
32. Peters, D., Peters, J. Quantum theory of the structure and bonding in proteins, part 8, the alanine dipeptide. J. Mol. Struct. 85:107–123, 1981.
33. Rose, I.A., Fung, W.-J., Warms, J.V.B. Proton diffusion in the active site of triosephosphate isomerase. Biochemistry 29:4312–4317, 1990.
34. Ramachandran, G.N., Sasisekharan, V. Conformation of polypeptides and proteins. Advan. Prot. Chem. 23:283–438, 1968.